

Atmospheric Potential-Gradient Measurements at Sea

S. G. GATHMAN AND EVA MAE TRENT

*Atmospheric Physics Branch
Ocean Sciences Division*

February 24, 1970



NAVAL RESEARCH LABORATORY
Washington, D.C.

CONTENTS

Abstract	ii
Problem Status	ii
Authorization	ii
INTRODUCTION	1
COMPARISON BETWEEN POTENTIAL AND FIELD MILL APPARATUS	2
POTENTIAL-GRADIENT MEASUREMENT	2
ATMOSPHERE-FOLLOWER COUPLING	11
THE CALCULATION OF CORRECTION FACTORS	12
STACK GAS MODEL	14
DETERMINATIONS OF THE REDUCTION FACTOR	16
ACKNOWLEDGMENT	17
REFERENCES	18

ABSTRACT

Shipboard measurements of atmospheric potential gradient are discussed. A comparison is made at sea between the performance of a potential-measuring apparatus and a field mill. The design of electrometer input multistage voltage followers is presented as a solution to the degradation of insulators by the salt environment. A model is given which calculates from the ship's engine power and the relative wind vector the potential gradient due to the charged stack gas. A method is also described by which a reduction factor can be calculated so that the geometric distortion of a ship's superstructure is accounted for in potential-gradient measurements.

PROBLEM STATUS

This is an interim report on the problem; work is continuing.

AUTHORIZATION

NRL Problem A02-15
Project RR 004-02-42-5150

Manuscript submitted November 25, 1969.

ATMOSPHERIC POTENTIAL-GRADIENT MEASUREMENTS AT SEA

INTRODUCTION

Atmospheric electrical measurements have been made predominantly over land since the days of Ben Franklin. Notable exceptions to this rule exist; for example, the results from the cruises of the *Carnegie* (1), *Horizon* (2), and *Meteor* (3). Blanchard's (4) discovery of the electrical charge carried by jet drops emanating from the bursting of minute air bubbles at the air-sea interface has generated renewed interest in oceanic atmospheric electricity. Small evaporating jet droplets are entrained by air currents near the air-sea interface and transported aloft by various atmospheric mechanisms.

Modern instruments are easily capable of measuring the atmospheric space charge with limiting sensitivities of the order of 50 to 100 elementary charges per cubic centimeter. Since the typical charge on the jet drops as they leave the ocean surface is in the order of 1000 electronic charges, the instruments can distinguish the remains of one jet drop in about 10 cc of air. Electrical measurements can thus be very sensitive detectors of jet drops. Sources of jet drops are easily distinguished in that they are associated primarily with white water patches on the air-sea interface. The transportation of these jet droplets from their sources of origin to a measurement platform is accomplished by atmospheric dispersion mechanisms.

Measurements of space charge made aboard the USNS *Eltanin* by Gathman and Trent (5) hint of the usefulness of this mechanism to indicate atmospheric stability. Here it was found that peaks in the measured space charge density occurred if, and only if, wave heights were great enough to produce whitecaps and a higher than normal humidity was observed, indicating that water vapor did come recently from the near air-sea interface. In other words, peaks in space charge were measured if there was a source of the jet drops and if an atmospheric mechanism existed to transport this charge from the air-sea interface to the measurement apparatus located on board ship.

The atmospheric electric field measured at the ocean surface by the *Carnegie* has shown the relationship of the maintenance of the earth's negative charge and worldwide thunderstorm activity. One unexplained phenomenon reported by all investigators at sea using different types of instrumentation concerns large fluctuations in the potential gradient with periods of from 2 to 12 min which occur even over glassy seas and are not related to the jet drop phenomenon.

An electrode effect is also known to exist over water (at least during periods of calm). The interrelationships between jet drop activity, electrode effect, and over-water atmospheric stability have yet to be determined.

As a prerequisite to an experimental investigation of these electrical air-sea interactions and associated phenomena, a systematic study of instrumental techniques and problems of shipboard atmospheric electrical measurements has been undertaken by NRL and is summarized in this report.

Problems arise in adapting instruments designed for measurements over land to instruments suitable for shipboard use. Degradation occurs on metallic surfaces and

sensor insulators because of the salt environment. A second and more troublesome problem is the effects caused by the ship itself. The geometric distortion of the electric field lines in the vicinity of the ship must be accounted for. An even more serious problem is the stack gas, normally positively charged (for diesel engines), which extends downwind in a plume superimposing its field on that of the measurement.

It is the purpose of this report to discuss these problems in detail and to suggest workable solutions. The report will be limited to the discussion of the electric-field measuring apparatus; however, the same field-measuring instruments may be used inside a Faraday cage to measure the atmospheric space charge, and many of the comments will be useful for both types of data.

COMPARISON BETWEEN POTENTIAL AND FIELD MILL APPARATUS

In early 1967 instruments measuring the atmospheric electric field by two different methods were placed aboard the USNS *Mizar*. They ran unattended except for changing chart paper during the cruise. One purpose of the experiment was to evaluate the dependability of the two methods at sea. The electric field was measured by an atmospheric-potential instrument (see following section) and by a field mill (6). Both instruments were exposed to the same artificial field, which was periodically made zero to allow for distinguishing variations in zero drift and gain stability. The artificial field applied to the two sensing devices was 85.8 V/m.

In an ideal experiment where both instruments are equally good, there should be no difference between the simultaneous outputs of both instruments if the same signal acts as an input to each. In this experiment, differences between the outputs of the two instruments did occur. It was assumed that the variations were the results of zero drift, gain instability, and in recording or reading errors. Zero drifts in potential-measuring instruments may be the results of specific tube characteristics; residual fields in the field mills are the predominant causes of the zero drifts. Variations in the gain stability are due in the former case to ion plume variations, which produce changes in the effective height of the potential probe. In field mills, gain stability may be influenced by temperature, humidity, and aging on the high-gain amplifier circuitry over relatively long periods of time. Since the reading equipment was the same in both methods, it can reasonably be assumed that the error would be approximately of the same magnitude in both cases.

A statistical analysis of the 696 hours of data was made. The standard deviation of the gain in the field mill was 18.32 V/m and that of the potential measuring apparatus was 6.86 V/m. The standard deviation of the zero drift in the field mill was 17.90 V/m and in the potential measuring instrument was 4.66 V/m. It is concluded that, since the NRL potential instrument showed a considerably smaller standard deviation in both gain stability and zero drift, it is better in those two respects than the field mill for long-term use. When the initial cost of instrumentation for the two methods is considered, the potential method is low compared to the other; maintenance also is less in that the radioactive sources can easily be changed, but metal corrosion causes problems in the field mill.

POTENTIAL-GRADIENT MEASUREMENT

It follows then that perhaps the best instrumental approach to the measurement of electric field at sea would be the potential-gradient method. Here all that is to be measured is a voltage which ranges between 1 and 1000 volts but at a very high source

impedance. The use of a radioactive element on the sensing antenna reduces the effective atmospheric impedance to about 5×10^{10} ohms. Therefore the voltmeter must have an input impedance large only with respect to this number. Electronically this calls for an electrometer voltmeter but with a much wider range of voltages than is available commercially.

There are two ways of making this measurement. One is the voltage divider method, which requires high resistances in a dividing network. The accuracy of the measurement depends on the constancy of the input resistor and the integrity of the input insulator. These sources of error make the voltage divider undependable at sea. The other approach is the use of an electrometer follower circuit where the low-impedance, high-voltage output is used as an insulator guard thereby effectively increasing the input impedance by a large amount. This approach holds the most promise for potential-gradient measurements at sea.

The obvious device for the measurement of voltage with an extremely high input impedance and low grid current, while at the same time being moderately unsusceptible to high-voltage spikes, is the electrometer tube. Unfortunately this device is limited in the voltage operating range that is required for our purposes. Thus some means must be used to employ an electrometer tube cathode follower with the high operating voltages that are found in potential-gradient measurements.

Two-stage feedback followers have been described by Brewer (7), Crozier (8), and Krakauer (9). These circuits, while effective, are limited to relatively small output currents (approximately $60 \mu\text{Amp}$) and voltage excursions of $\pm 600 \text{ V}$. A working NRL model of this kind of follower is shown in Fig. 1. A voltage-sensitive device which will tolerate much larger output currents is necessary for long-term operation at sea because of the problem of salt spray short circuiting all unguarded insulators. A large bipolar voltage swing is also required to allow the device to follow the potential variations in the atmosphere during all types of weather. In order to accommodate these requirements, the following extension of the feedback principle was incorporated.

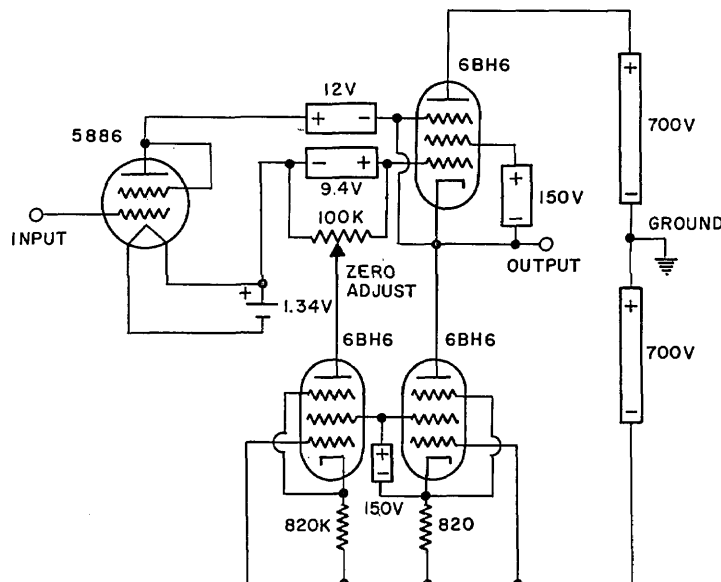


Fig. 1 - Two-stage follower with $\alpha = 0.003$, output voltage range of $\pm 600 \text{ V}$ at $60 \mu\text{Amp}$

A voltage follower may be represented by a three-terminal triangle as in some later figures. One of the vertices is considered the reference ground terminal, another the low-impedance output terminal. On the side of the triangle opposite the output vertex will be shown the high-impedance input terminal. The output voltage with respect to the ground terminal is essentially the same as that on the input terminal. In describing the performance of the circuit, we may write $V_{\text{output}} = (1 - \alpha) V_{\text{input}}$, where the effective gain of this triangle is $(1 - \alpha)$ or essentially unity if α is small.

When three essentially unity-gain followers are cascaded as shown in Fig. 2, three outputs, O_1 , O_2 , and O_3 , are available with current output capabilities and impedance levels of the followers F_1 , F_2 , and F_3 , respectively. The effective voltage gains at these outputs, however, are $1 - \alpha_1 \cdot \alpha_2 \cdot \alpha_3$, $1 - \alpha_2 \cdot \alpha_3$, and $1 - \alpha_3$ where α_1 , α_2 , and α_3 are the differences between unity gain and the actual gains of the individual followers. Furthermore the voltage range of F_1 must only be adequate to cover the error in F_2 , and similarly the voltage range of F_2 must only be adequate to cover the error in F_3 . Thus, only F_3 must have a high-voltage capability.

Multistage voltage followers may then be built up from a collection of various types of special-purpose unit voltage followers to satisfy particular needs. As there was no existing general-purpose voltage follower that answers all the needs for all types of investigations simultaneously, a collection of special-purpose followers was developed by NRL and is briefly described below. Combinations of these instruments may be made to fit various applications either on board ship or elsewhere. One problem associated with this approach is the number of individual, isolated, power supplies needed to operate the various unit voltage followers in the three positions of Fig. 2. This may be accomplished by batteries and/or power-line isolation transformers.

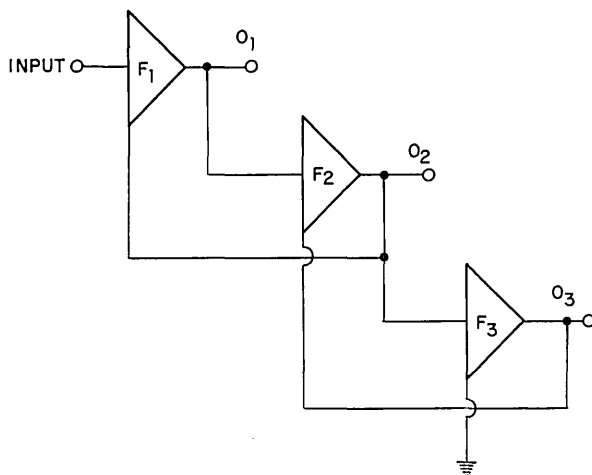


Fig. 2 - Multistage follower constructed from simple stages

In voltage-follower work, it has been found necessary to use some sort of antenna equalizer and not to depend on natural atmospheric conductivity to dissipate the charge on the antenna system (10). As this charge can be brought to the antenna not only by grid current from the input electrometer tube but also by charged atmospheric dust and sea salt nuclei, etc., it is of the utmost importance to dissipate it as rapidly as possible to avoid changes in the measured input voltage. Consequently ultralow grid-current

characteristics are not required for this application, and an adequate input stage may be constructed from a triode-connected electrometer tube operated as a simple cathode follower as long as it is operated in the region where the grid current is on the order of 10^{-13} A or less so that it may be easily dissipated by the antenna equalizer.

A typical circuit utilizes the 5886 electrometer tube. As we are concerned mainly with dc, or at most, low audio-frequency signals, the parameters which are most important here are input resistance, input grid current, output impedance, and output voltage swing. Figure 3 shows the input electrometer tube mounted inside a hermetically sealed aluminum head box. The high-impedance parts of this circuit are all enclosed in this box, which also has a cavity filled with a desiccator to keep the relative humidity as low as possible. This is a partial requirement for low-grid-current operation. The manufacturer's characteristics of the 5886 in the triode connection show that for the recommended plate current of $200 \mu\text{A}$, the positive supply voltage of between 9 and 18 V offers adequately low grid currents between $\pm 2 \times 10^{-13}$ A. Connections to the other parts of the

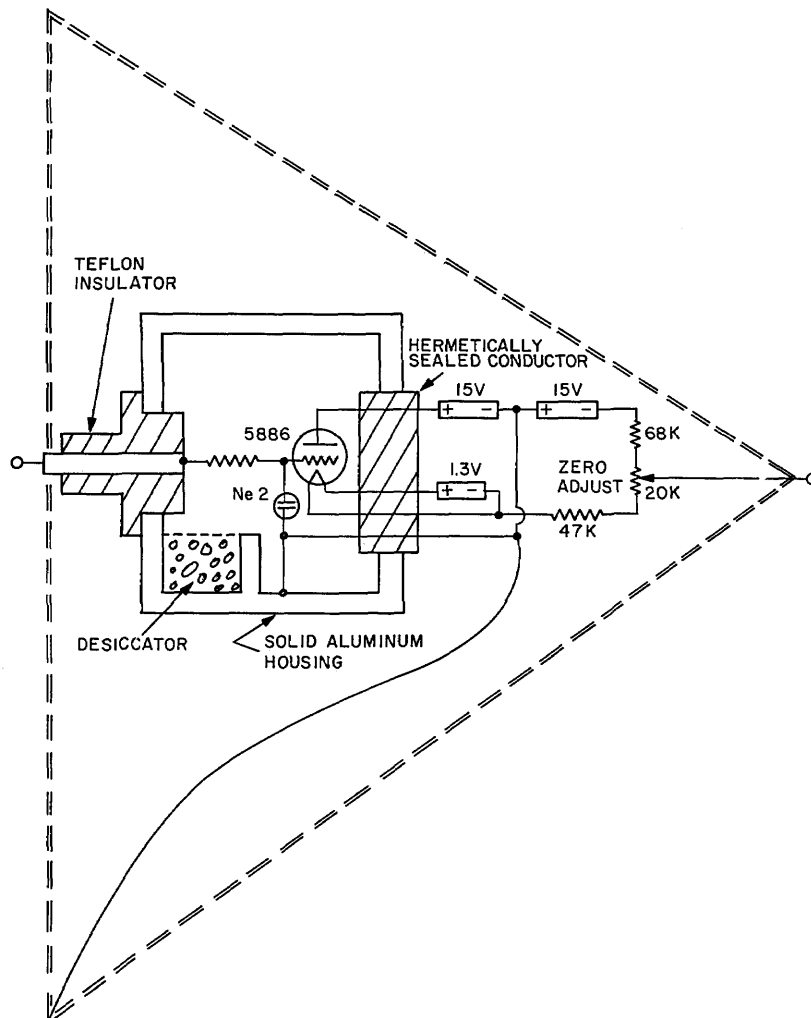


Fig. 3 - F_1 input stage showing hermetically sealed construction, input overload protection, and zero adjustment. The α of this stage is 0.4, and the output voltage swing is about $\pm 3\text{-}1/2$ V; however, the input impedance is very high and the grid current less than 2×10^{-13} A.

circuit are made by means of a hermetically sealed connector and an ordinary multiconductor control cable.

The shell of this head box is kept at the output voltage of the system; thus for a good voltage follower all capacitive and resistive loading across the large Teflon input insulator is reduced by the feedback principle. In effect, the input parameters of most importance become the input grid current and the unsusceptibility to instantaneous input-voltage spikes.

The protective system shown in Fig. 3 consists of a common composition resistor and a type NE-2 neon glow bulb. The leakage resistance across the recently cleaned NE-2 has been measured to be in excess of 10^{12} ohms and the shunt capacity as less than 1 pF. By connecting the neon bulb to the common terminal of F_2 rather than to ground, the effective leakage and capacity values are improved significantly. In practice, any loading of the input due to the neon lamp has been undetectable. In normal operation, the output of F_2 relative to its common terminal is only a few volts and nowhere approaches the ignition potential of the neon bulb. The bulb responds to transient overloads in a fraction of a millisecond, however, thus protecting F_1 .

The intermediate stages are most easily constructed by using commercially available operational amplifiers. Since the accuracy of the system strongly depends upon the characteristics of this unit, the "burden of proof" is thrust in great measure to the amplifier supplier. As the input device is deficient in both gain and output voltage swing, the intermediate stage must correct these deficiencies and at the same time be capable of driving the output or last stage.

Figure 4 shows a device which is designed to have a power supply in common with the input stage. The operational amplifier can be any of a number of economy-grade, ± 10 V, general-purpose, operational amplifiers. Most of these devices have input impedances sufficiently high so as not to overload the input stage. Their gain is very high, so that the input stage operates at essentially its quiescent point at all times. Its output is usually ± 10 V at 10 mA which is sufficient to drive most of the last-stage followers described below.

A second type of intermediate stage follower is described in Fig. 5. This device utilizes a high-voltage differential operational amplifier, usually ± 100 V, such as the Philbrick tube, type SK2-V. (Many solid-state, high-voltage, operational amplifiers have limitations on the maximum common-mode voltage that can be applied across their inputs and therefore their usefulness as voltage followers is severely limited.) This design has an output of a sufficient voltage magnitude to be adequate for many purposes in

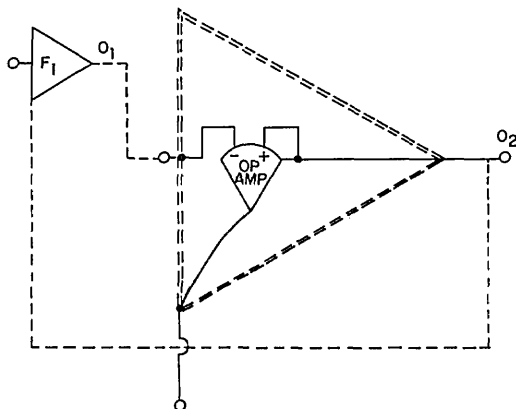


Fig. 4 - F_2 intermediate stage follower constructed from a commercial transistorized operational amplifier. The chief advantage to this design is that the F_1 and F_2 circuits may share a common power supply. The α of this stage is always very small depending on the amplifier used, whereas the output is usually capable of ± 10 V at 10 mA.

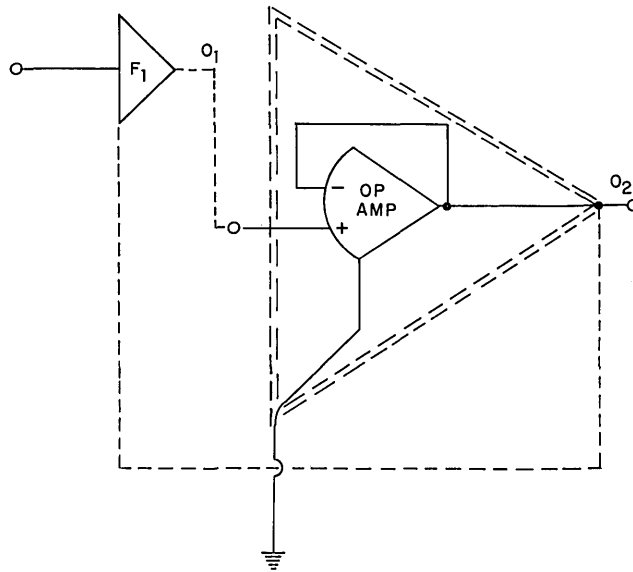


Fig. 5 - An alternate F_2 intermediate stage using a differential input operational amplifier

itself and can be considered as the final stage. It is also useful as an intermediate device for slowly responding, high-voltage final stages in that it will rapidly respond to as much as ± 100 V variation about the output level of the final stage.

The greatest problem in high-voltage following circuits is encountered in the final (F_3) stage, where high voltage and high current capabilities must be maintained, while at the same time aiming at rapid bipolar response with a minimum of wasted power. Several devices are described below which meet some, but not all, of the above requirements. In the present state of the art, it is up to the instrument designer to make the correct compromise between characteristics and to choose an appropriate device. With a good intermediate stage, however, this stage can be relatively inaccurate without undue compromise of the overall system performance.

A simple high-power follower based upon a motor-driven autotransformer within a servo loop has been used with success. The output range and current capability are dependent only on the capacity of the transformers and rectifiers used and may be made as large as necessary. The autotransformer supply pictured in Fig. 6 has a capacity of 1700 V at 100 mA. Thus in the field, output O_2 is used when a high-precision voltage is needed at less than 10 mA. When high power is required and accuracy is not so important, O_3 is used. The chief problem in this approach is that the output is of one polarity only. Zero crossing can only be done by mechanically switching high-voltage leads.

When zero crossing must be done rapidly and automatically, an alternative approach is to use thyratrons to rectify an ac voltage, controlled in such a way that they act as a voltage follower. Figure 7 shows a simplified diagram of such a follower. The input is compared with the output by means of a mechanical chopper. The resultant ac voltage is fed into a synchronous rectifier, the single-ended output of which produces a dc error signal. This in turn is compared with a ramp voltage in phase with the 60-Hz line by a voltage comparator. The resultant pulse train is then fed into two AND gates together with a suppression pulse and polarity-steering voltages. The resulting time-related pulses are directed to the appropriate thyatron. Thus the greater the error of either

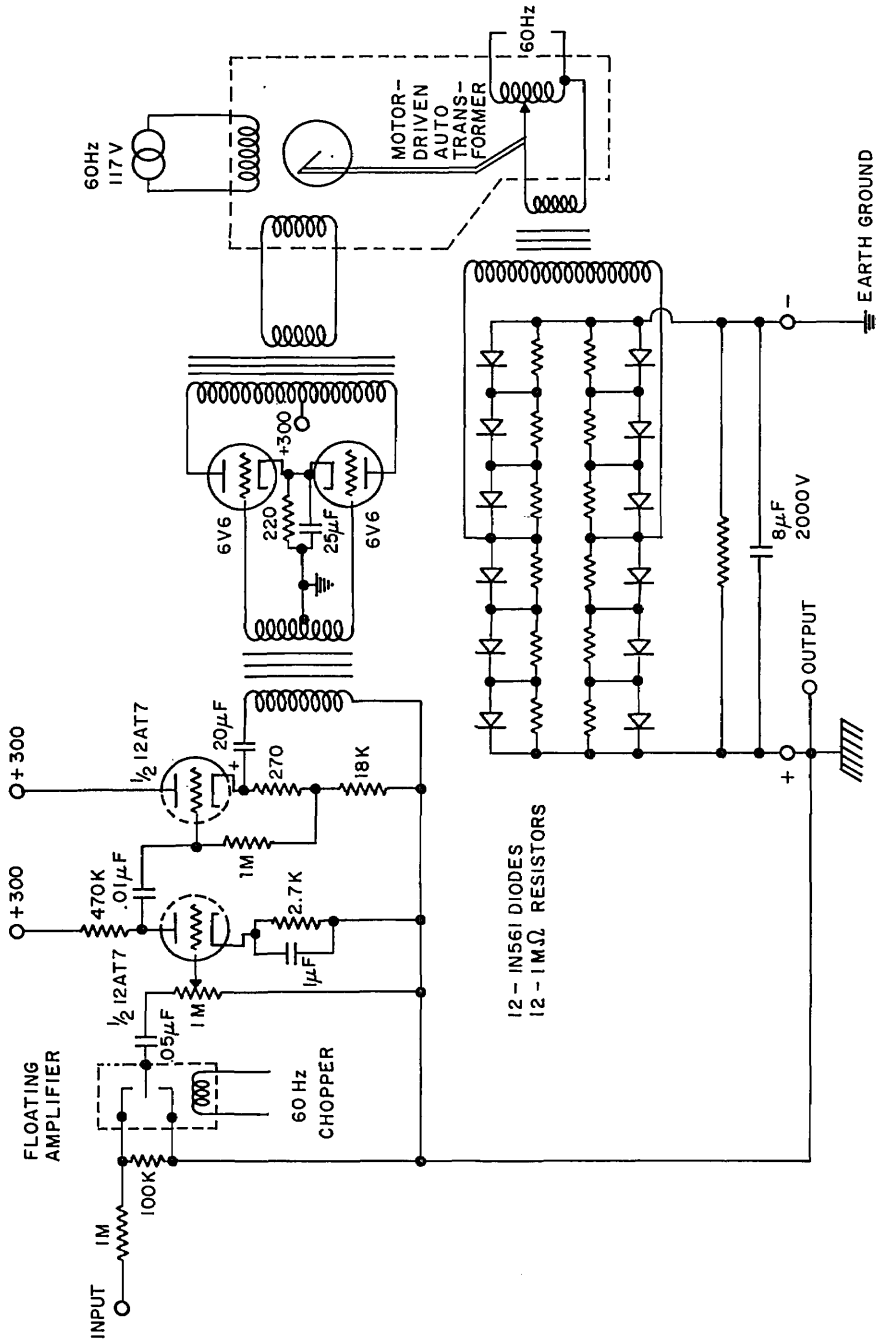


Fig. 6 - A unipolar F_3 final stage featuring high-voltage and high-current output using a motor-driven autotransformer in a servo loop

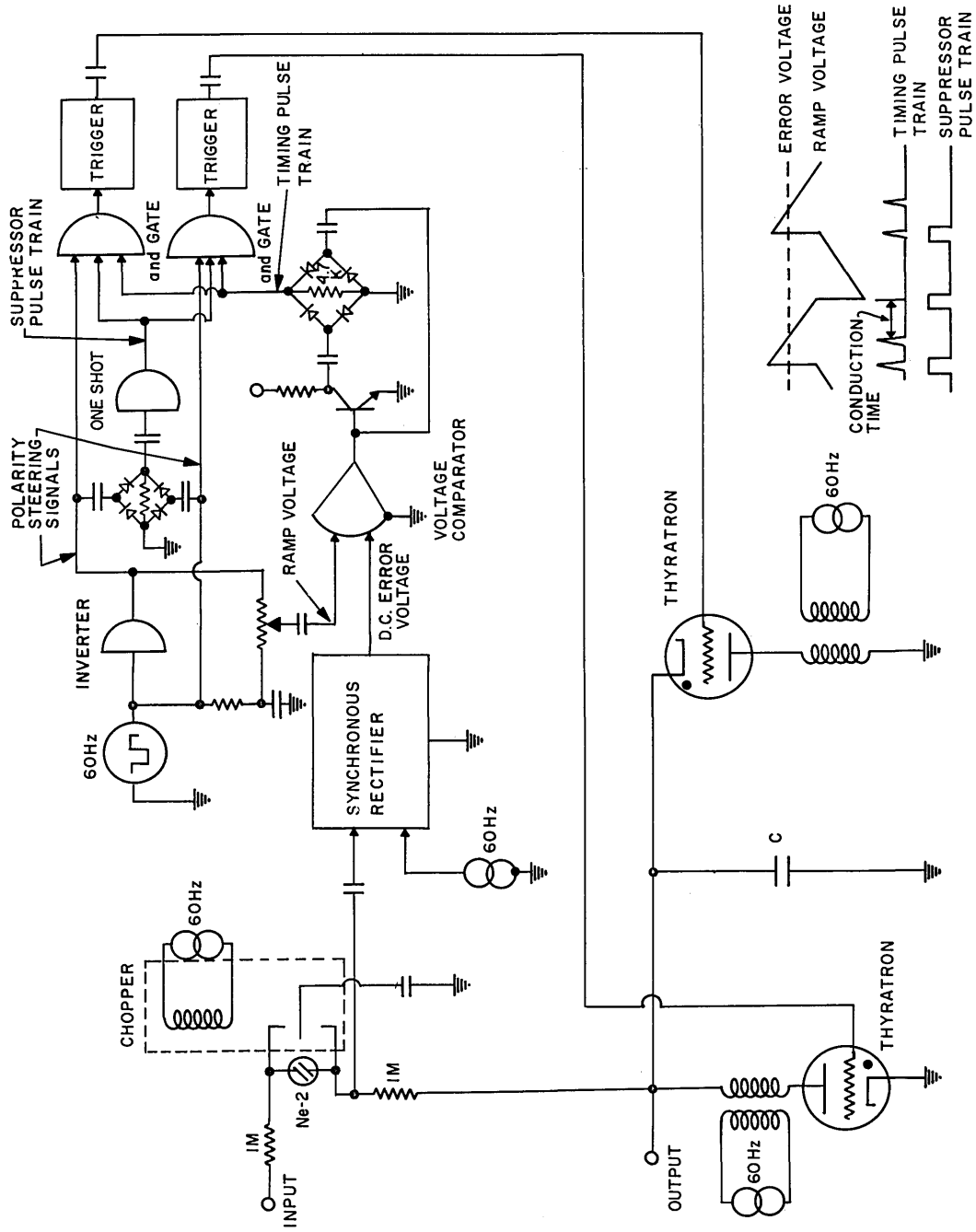


Fig. 7 - A bipolar F_3 final stage incorporating two thyratrons to maintain a charge on capacitor C such that the output voltage is almost equal to that of the input

polarity, the earlier the correct thyatron is fired that results in more charge being applied to the output capacitor. The advantages of such a device are that for dc voltage-following applications, high voltages of both polarities may be obtained. The trigger-control circuitry is easily made using commercially available analog and digital modules and may be separated from the high-voltage sections.

Another instrument has been developed which is somewhat similar to the thyatron circuit but may be battery operated. This circuit uses relays which are switched on and off by means of an error signal. These relays then maintain a charge on a capacitor by connecting positive and negative high-voltage batteries through resistors such that the voltage across the capacitor is very close to the input voltage. This circuit as shown in Fig. 8 can be built using high-voltage reed relays which allow very high-voltage operation, the voltage drop being across only the high-voltage terminals of the relays and the capacitor. The speed of operation of the system is a function of the speed of the relays and of the ability of the high-voltage batteries to supply current to the main capacitor.

Another device, shown in Fig. 9, utilizes a high-voltage, high-current, cathode follower made with transmitting tubes. It has been combined with a second floating follower in the manner described by Gathman and Anderson (6) to obtain a very low output impedance. Although this device does not exceed the two-stage cathode follower in the voltage range described earlier, its output current is greatly increased.

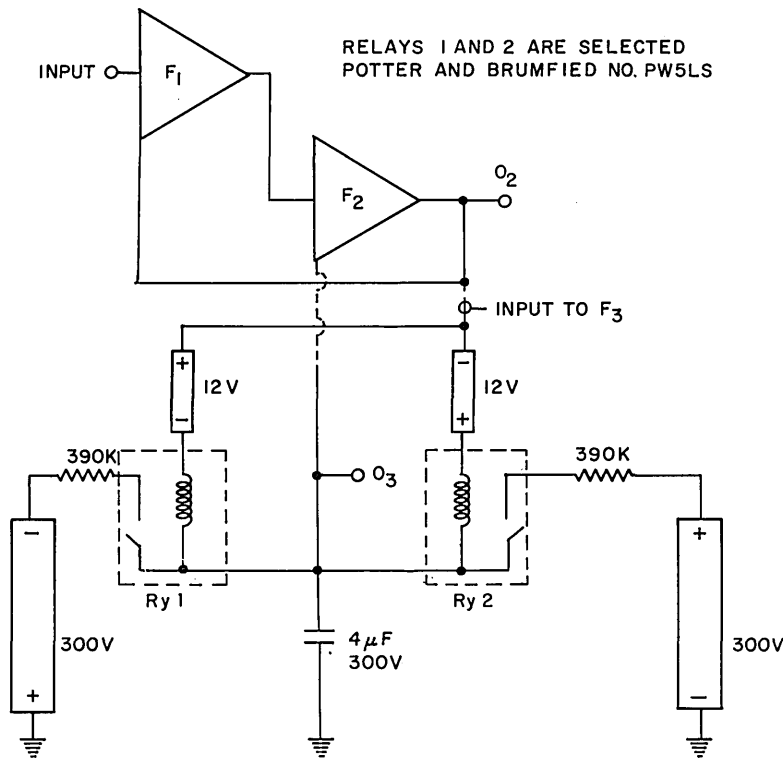


Fig. 8 - A relay type F_3 final stage incorporating two relays to switch positive and negative current into the $4\mu\text{F}$ capacitor in order to maintain an output voltage almost equal to that of the input. The device is ideal for remote field operation where low-power battery operation is essential. It is shown here connected with the F_1 and F_2 stages.

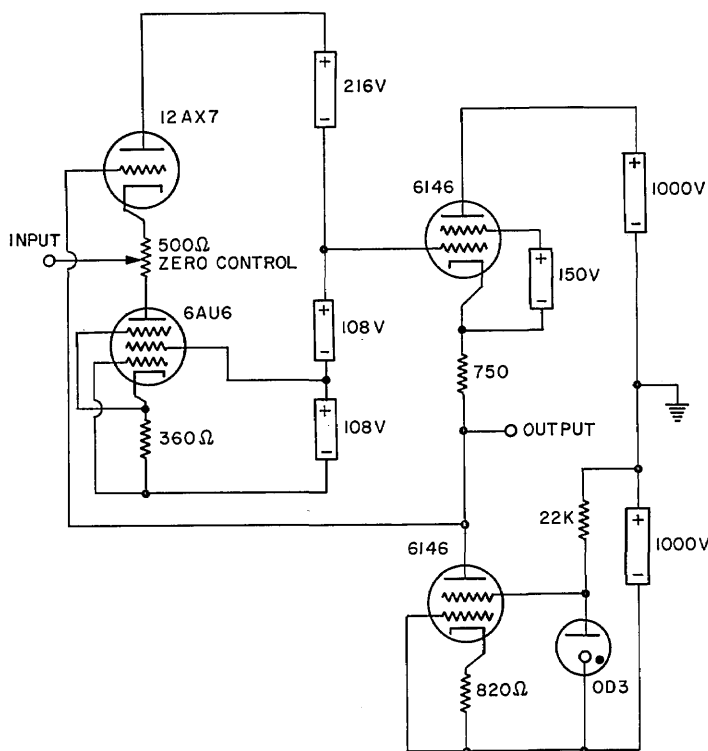


Fig. 9 - An output F_3 stage incorporating transmitting tubes. This device has a very low output impedance and can deliver 10 mAmp of current in a voltage range of ± 600 V.

Manufacturers supply operationally programmable power supplies which may be used as last-stage devices, but these devices are of one polarity only, and of the devices that have been examined only negative outputs are available, which make them essentially useless for atmospheric electric field work without extensive modification.

ATMOSPHERE-FOLLOWER COUPLING

Figure 10 is a schematic which shows a realistic voltage follower coupled to the true atmospheric potential V_a through an antenna resistance R_a and with an antenna capacity to ground of C_a . The follower is assumed to have a gain of $1 - \alpha$ and a high input impedance. To minimize resistive and capacitive losses encountered in the input insulator, the antenna is guarded by the output voltage which is almost that of the input. The capacity and the leakage resistance across this insulator are represented by R_f and C_f . A follower has a zero offset which is represented by the battery ϵ , and the existence of grid current is accounted for by I_g . By applying Kirchoff's law and setting the algebraic current into point A to zero, we may obtain the differential equation involving the voltage of point A to ground as

$$\frac{dV}{dt} = - \frac{\left(1 + \frac{\alpha R_a}{R_f}\right) V}{R_a(C_a + \alpha C_f)} + \frac{V_a - \frac{R_a}{R_f} \epsilon (1 - \alpha) - I_g R_a}{R_a(C_a + \alpha C_f)}$$

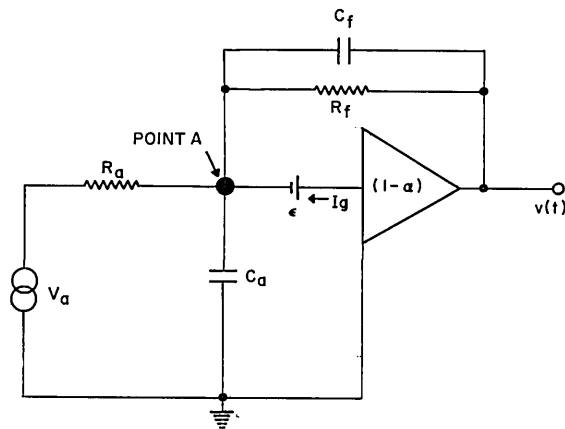


Fig. 10 - A realistic voltage follower coupled to the atmospheric potential V_a by an antenna of capacity C_a through a source impedance R_a

With a boundary condition that at $t = 0$, $V = 0$ (this is accomplished by initially shorting the antenna to ground), the voltage at the output of the follower $v(t)$ is given as

$$v(t) = \frac{(1-\alpha)}{1 + \frac{\alpha R_a}{R_f}} \left[V_a - \frac{R_a}{R_f} \epsilon (1-\alpha) - R_a I_g \right] \left\{ 1 - \exp \left[-t \frac{\left(1 + \alpha \frac{R_a}{R_f} \right)}{R_a (C_a + \alpha C_f)} \right] \right\} - \epsilon (1-\alpha) .$$

For $\alpha \ll 1$ this becomes

$$v(t) = \left(V_a - \frac{R_a}{R_f} \epsilon - R_a I_g \right) 1 - \exp \left(- \frac{t}{R_a C_a} \right) - \epsilon .$$

The parameters R_a , R_f , I_g , and ϵ are obviously important in the correct operation of this device.

Ordinarily type 5886 electrometer tubes are easily operated with their grid currents less than 10^{-13} A. If Po^{210} sources are used as potential equalizers, the effective coupling resistance is about 5×10^{10} ohms for source strengths of $250 \mu\text{Ci}$. Thus the grid current term will be only 5 mV and completely negligible when compared with the atmospheric potential V_a . The voltage offset ϵ ordinarily is not a problem, but when the input insulator becomes contaminated in operation, the term R_a/R_f can greatly multiply the effect of the offset voltage and make it comparable to or greater than the atmospheric potential.

In operation it is usually wise to simulate periodically the atmosphere with a 10^{11} -ohm resistor and a high-voltage battery to ascertain the trustworthiness of the device in use.

THE CALCULATION OF CORRECTION FACTORS

It is a law of electrostatics that lines of electric force approach conducting bodies normal to the surface of the conducting body. Thus a ship floating on the surface of the

sea greatly affects the geometry of the electric field in its vicinity. Electric fields measured on the deck of the ship are not equal to the electric fields that would be at that point were the ship not there, and measurements of the electric field from the deck of the ship must be corrected for this distortion if these measured values are to relate to any other measurement of the electric field. The determination of this reduction factor, which will allow an undisturbed field to be computed from a measurement of a disturbed field, is particularly difficult for ship measurements. All measurements of the electric field must be referred to those made over a flat plane. Some way must be found to compare simultaneous readings of an electric-field meter mounted on a ship with an electric-field meter mounted on a plane, presumably on land or on a quiet sea surface.

The atmospheric electric field is the superposition of fields from various sources ranging from a worldwide to a local scale. To compare two field-sensitive instruments, it is best to locate these instruments as close together physically as possible in order to measure simultaneously the same electric field. It has been found that this is by no means an easy task. Gathman and Trent (11) have shown that even in ideal field site conditions, the ratio of measurements between a flush-mounted, electric-field mill located in the ground plane (considered as the standard) and an identical instrument mounted nearby on a boom from an instrumentation shack varied $\pm 19.3\%$.

Difficulties occur when trying to compare on-shore measurements with those made simultaneously at sea. Over the oceans within the boundary layer, meteorological conditions are remarkably similar from place to place as shown by Brocks (12) when high correlations between simultaneous measurements of meteorological parameters were made within a sea area of dimensions in the order of 50 km. However, inland of the surf zone, conditions change and the electric field varies with height and position within the lowest layers of the atmosphere and depends on local space charge sources, distributions, and movements. Factors which have strong local effects are air pollution, ionization rate, surf and white water, turbulence, and storm centers.

A system that minimized these local sources of error was devised for the calibration of the USNS *Mizar*. The first phase of the calibration was carried out in the Atlantic Ocean. The ship was operating on several stations near Barbados, West Indies. The weather conditions were mostly fair, and a steady east wind of about 10 knots was constant throughout the period. There were few whitecaps in the sea surface, and the resultant minimum amount of jet drops to confuse the picture was confirmed by the use of Faraday cages. The electric field was measured by the potential-gradient apparatus shown in Fig. 11 mounted on the outside of the Faraday cage on top of the well house of the USNS *Mizar*. This apparatus was continuously recording while being monitored by scientific personnel during the period of measurement.

Identical instrumentation was installed on the *Lone Ranger*, a small wooden fishing boat based out of Bathsheba, Barbados, shown in Fig. 12. The cage bottom was about 2 ft above the mean waterline of the boat. The small protrusion of the cabin above the base of the cage level was so small as to be considered negligible on the field measurement. The boat was moored to a buoy about 1000 yd outside of the surf zone and the atmospheric electrical equipment operated on batteries. It was also continuously recording, and the instrumentation monitored by scientific personnel.

Only one battery-operated potentiometric recorder was available on board the *Lone Ranger*. As a result, it was necessary to alternate the recorder between the electric field and the Faraday cage instrumentation. The usual procedure was to switch the recorder at 1/2-hour intervals.

Simultaneous recordings on the USNS *Mizar* and the *Lone Ranger* were taken on April 16, 17, and 18, 1969. Station I of the ship was located at $15^{\circ}24'N$ and $59^{\circ}55'W$ with

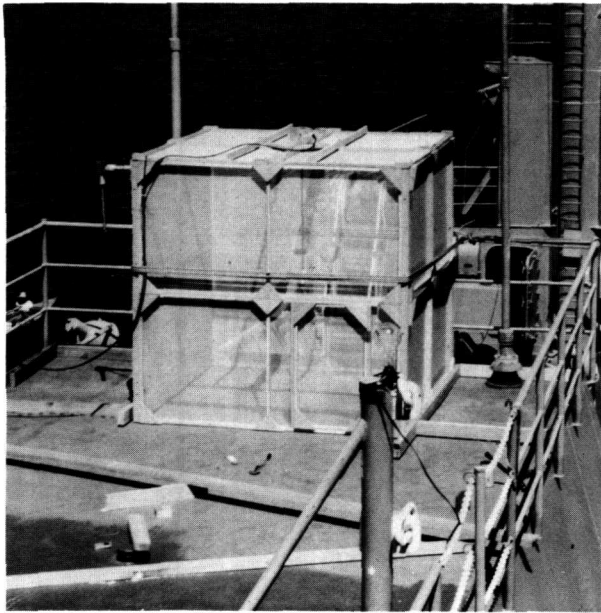


Fig. 11 - The installation of the potential-gradient instrument on the side of the Faraday cage aboard the USNS *Mizar*



Fig. 12 - The installation of the potential-gradient instrument and Faraday cage on the *Lone Ranger*

a bearing of 350 degrees from the buoy and a distance of 133 naut mi. Station II was located at $13^{\circ}14'N$ and $59^{\circ}8'W$ with a bearing from the buoy of 87 degrees and a distance of 22 mi. Station II was occupied on April 17 and 18, 1969.

During Station II, a unique opportunity presented itself to compare the effects of motion on the electric field measurement on board the ship. A short run was made by the USNS *Mizar* to and from the point $13^{\circ}6-1/2'N$ and $59^{\circ}22'W$. The point of closest approach to land had a bearing of 126 degrees and a distance of 11 naut mi from the buoy. Throughout this whole period, the instrumented fishing boat was monitoring the atmospheric electric field and space charge.

Diesel exhaust, one local effect, is known to contain a positive charge (13). As such it superimposes a locally produced component on the earth's field. In order to determine just how this field produced by stack gas would vary at a typical measurement point on the ship as a function of wind speed and direction, the following model was used.

STACK GAS MODEL

Consider Fig. 13, where the charged stack gas is represented by a horizontal line of positive-charge centers of charge q located a distance a apart. This line of charge emanates from a stack of height h located at the origin of the coordinate system. The direction is represented by ϕ , which is the angle between the projection of the line of charge on the horizontal plane and the coordinate representing the center line of the ship. The electric field s , due only to that of the charged stack gas and measured at a distance b from the stack on the center of the ship, is given by

$$s(a, b, h, \phi) = \frac{q}{2\pi\epsilon_0} \sum_{i=0}^{\infty} f_i(a, b, h, \phi) = \frac{qh}{2\pi\epsilon_0} \sum_{i=0}^{\infty} (b^2 + h^2 - 2abi \cos \phi + i^2 a^2)^{-3/2}. \quad (1)$$

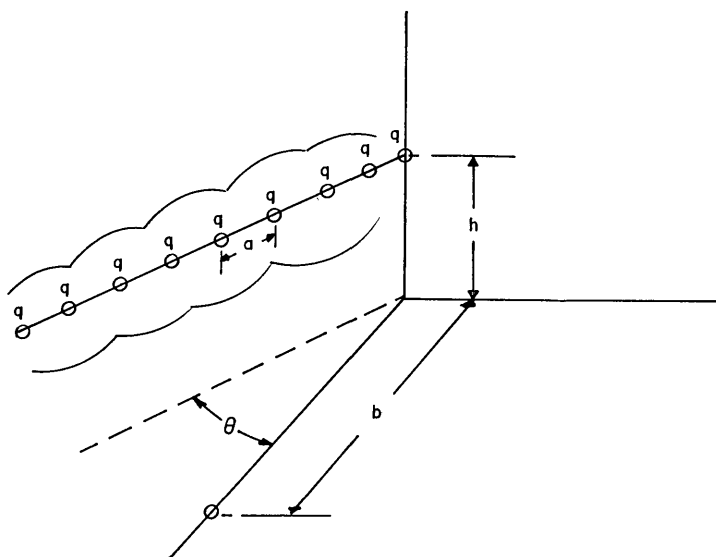


Fig. 13 - A diagram of the stack-gas model showing the spatial parameters

The maneuver by the USNS *Mizar* on April 17, 1969 to and from the island of Barbados provided an excellent opportunity to estimate just how effective this model is at predicting the measured electric field on board the ship due to the charge concentration in the stack gas. During the first leg of this maneuver, the relative wind at the ship was toward 102 degrees, measured from the bow, with a speed of 6 knots, and the electric field had an average measured value of 240 V/m (Case I). The return leg provided a relative wind toward 200 degrees at 25 knots with an average electric field of 113 V/m (Case II). During Station II, the average electric field was 84 V/m, and the relative wind was toward 270 degrees at 10 knots. During Station II, of course, the stack-gas emanation was sharply decreased compared with the conditions under cruise power, the only power conversion being for electricity and air conditioning.

The ratio of the measured fields at the ship's measurement site for the two legs of the maneuver and due only to the effect of the charged stack gas is given by

$$R_d = \frac{240 - E}{113 - E},$$

where E is the component of the atmospheric electric field. The third measured component of the field, that due to the stack gas during the station when the ship's generators were producing minimum stack gas, is $84 - E = S'$. If we can assume that the ratio of the two cases for the field from the stack-gas model R_m is the same as the ratio of the data R_d , then the atmospheric field E may be computed and the field S' due to the stack gas during Station II may also be estimated;

$$R_m = \frac{s(3, 20, 20, 102^\circ)}{s(12, 20, 20, 200^\circ)} = 4.45.$$

Here, the distance a in meters is set proportional to wind speed by $a = u/2$, where u is expressed in knots.

If R_m is assumed equal to R_d , then E , the component of the atmospheric electric field, is 78 V/m. Thus $S' = 6$ V/m and s for Case I is 162 V/m. The charge q_I for the magnitude of charge centers in the model for Case I then may be obtained from Eq. (1) as

$$q_I = \frac{2\pi\epsilon_0 \times 162}{\sum_{i=0}^{\infty} f_i(3, 20, 20, 100^\circ)} = 1.2 \times 10^{-6} \text{ coulomb.}$$

The charge q_{III} obtained for Station II data and the reduced-engine operation is given by

$$q_{III} = \frac{2\pi\epsilon_0 \times 6}{\sum_{i=0}^{\infty} f_i(5, 20, 20, 220^\circ)} = 0.6 \times 10^{-7} \text{ coulomb.}$$

A rough rule of thumb presents itself when comparing these charges with power conversion. For lack of better information, one may logically assume that the charge in the stack gas is then proportional to the horsepower being generated and may deduce that 1 hp will produce charge centers for this model of 0.35×10^{-9} coulomb. These charge centers will be spaced a distance a apart.

An example of the application of the model to predict the electric field at a site on another ship produced by stack gas is shown in Fig. 14. These data are taken from cruise 31 of the USNS *Eltanin*, which was en route between San Francisco and Pago Pago during November and December 1967. The electric field was measured throughout this portion of the cruise. There were problems associated with the measurement of unexpectedly high electric fields. The broken line shows the normalized electric field values as a function of an independent parameter. (The electric field is obtained from averages taken over each 5-degree-latitude portion of the cruise.) The solid line represents the normalized electric field predicted by the stack-gas model which uses simultaneously obtained measurements of the relative wind speed and direction together with the horsepower being generated by the ship's diesel engine. The figure shows a strong correlation between the two curves (correlation coefficient = 0.89), indicating that the electric field was dominated throughout the cruise by the presence of the ship's stack gas.

DETERMINATIONS OF THE REDUCTION FACTOR

The reduction factor K_m is defined as the factor by which an indicated atmospheric electric-field measurement on a ship must be multiplied to reduce it to the field that would be present were the effects of the ship's geometry not important.

The ratio between the atmospheric electric field measured on the USNS *Mizar* (the effects of the stack gas are removed from the measurement) to the electric field seen by the apparatus on the *Lone Ranger* will be described as a relative reduction factor $K_{m,\ell}$. An additional reduction factor $K_{\ell,p}$ must be evaluated which is the ratio of the cage-mounted field meter apparatus to that made on a level plane. Thus $K_m = K_{m,\ell} \times K_{\ell,p}$ is the reduction factor for the USNS *Mizar*.

The three days of measurement off Barbados Island provided three different measures of $K_{m,\ell}$. They were respectively 0.43, 0.46, and 0.46. Inasmuch as the distance factor for Station I was larger than that for Station II, it seems reasonable to conclude that the relative reduction factor is 0.46.

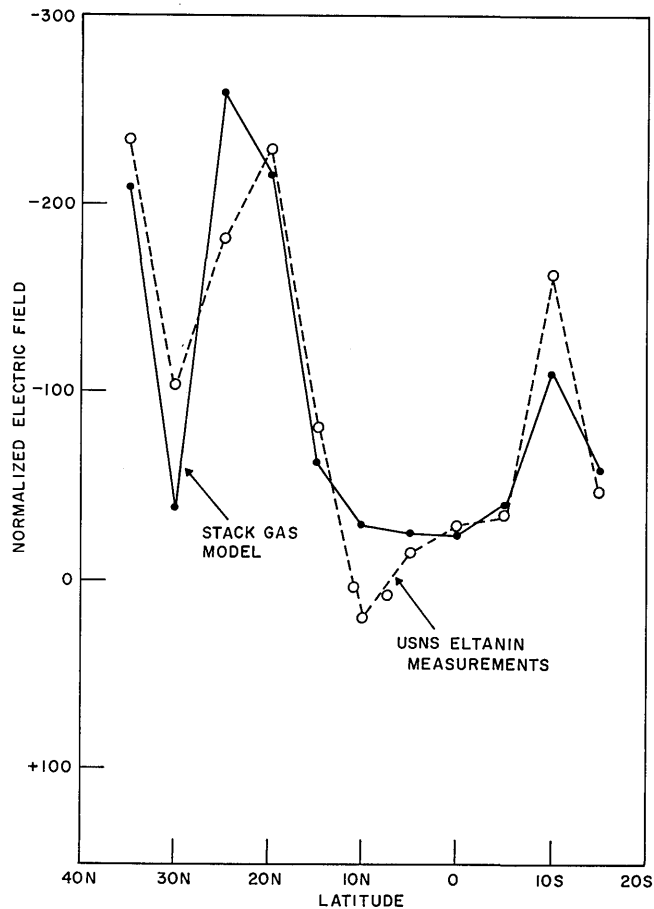


Fig. 14 - A comparison between the measured electric field aboard the USNS *Eltanin* as a function of latitude and the stack-gas field computed from the stack-gas model

An experiment was carried out on September 17, 1969 at the Waldorf, Maryland, annex to NRL. At this time over a level asphalt plane, both the cage-mounted field meter and an undistorted potential-gradient meter were read simultaneously every minute for a period of an hour. During this time the atmospheric electric field varied between 100 and 159 V/m and the average $K_{e,p}$ was $1.02 \pm 4\%$. It is therefore concluded that the reduction factor for this instrumentation mounted on the USNS *Mizar* is 0.47.

Other methods have been carried out for the determination of reduction factors for ships. Mühleisen (3) used a raft on the sea for his reduction factor determination on the *Meteor*. Ruttenberg and Holzer (2) were fortunate in finding a quiet lagoon where simultaneous measurements were made on the beach and on the ship. Caution must be exercised in the latter approach, however, because of the large amount of electrification that occurs with surf activity.

ACKNOWLEDGMENT

We thank Mr. Ben Julian of NRL and Mr. Jerome Forde, the captain of the *Lone Ranger*, for their help in obtaining the electric measurements near Barbados.

REFERENCES

1. Mauchly, S.J., "Studies in Atmospheric Electricity Based on Observations Made on the Carnegie, 1915-1921," *Researches of the Department of Terrestrial Magnetism, Ocean Magnetic and Electric Observations, 1915-1921*, V (175):384, Washington, D.C.: Carnegie Inst. of Wash.
2. Ruttenberg, S., and Holzer, R.E., "Atmospheric Electrical Measurements in the Pacific Ocean," in *Proc. Conference on Atmospheric Electricity, Wentworth-by-the-Sea*, edited by R.E. Holzer and W.G. Smith, I:101-108
3. Mühleisen, R.P., "Recent Potential Gradient and Ion Measurements on the Atlantic Ocean in 1965," *Fourth International Conference on the Universal Aspects of Atmospheric Electricity, 1968, Tokyo, Japan*
4. Blanchard, D.C., "The Electrification of the Atmosphere by Particles from Bubbles in the Sea," in "Progress in Oceanography," Vol. I, edited by Mary Sears, p. 71
5. Gathman, S., and Trent, E.M., "Space Charge over the Open Ocean," *J. Atmos. Sci.* 25 (No. 6):1075-1079, Nov. 1968
6. Gathman, S.G., and Anderson, R.V., "Improved Field Meter for Electrostatic Measurements," *Rev. Sci. Instr.* 36 (No. 10):1490-1493 (1965)
7. Brewer, A.W., "An Electrometer Valve Voltmeter of Wide Range," *Rev. Sci. Instr.* 30:91-92 (1953)
8. Crozier, W.D., "Measuring Atmospheric Potential with Passive Antennas," *J. Geophys. Research* 68:5173-5179 (1963)
9. Krakauer, S., "Electrometer Triode Follower," *Rev. Sci. Instr.* 24:496-500 (1953)
10. Dolezalek, H., "Passive Antenna and Collector Antenna for the Measurement of the Atmospheric Electric Potential," *J. Geophys. Research* 68:5181 (1963)
11. Gathman, S.G., and Trent, E.M., "Absolute Electric Field Measurements Using Field Mills," *NRL Report 6538*, 1967
12. Brocks, K., "Probleme der maritimen Grenzschicht der Atmosphäre," *Ber. Deut. Wetterdienstes* 91:34-46 (1963)
13. Mühleisen, R., "Die Luft elektrischen elements in Grosstadt bereich," *Z. Geophys.* 29:142-160 (1953)

DOCUMENT CONTROL DATA - R & D

(Security classification of title, body of abstract and indexing annotation must be entered when the overall report is classified)

1. ORIGINATING ACTIVITY (Corporate author) Naval Research Laboratory Washington, D.C. 20390		2a. REPORT SECURITY CLASSIFICATION Unclassified	
		2b. GROUP	
3. REPORT TITLE ATMOSPHERIC POTENTIAL-GRADIENT MEASUREMENTS AT SEA			
4. DESCRIPTIVE NOTES (Type of report and inclusive dates) This is an interim report on the problem; work is continuing.			
5. AUTHOR(S) (First name, middle initial, last name) Stuart G. Gathman and Eva Mae Trent			
6. REPORT DATE February 24, 1970		7a. TOTAL NO. OF PAGES 22	7b. NO. OF REFS 13
8a. CONTRACT OR GRANT NO. NRL Problem A02-15		9a. ORIGINATOR'S REPORT NUMBER(S) NRL Report 7030	
b. PROJECT NO. RR 004-02-42-5150			
c.		9b. OTHER REPORT NO(S) (Any other numbers that may be assigned this report)	
d.			
10. DISTRIBUTION STATEMENT This document has been approved for public release and sale; its distribution is unlimited.			
11. SUPPLEMENTARY NOTES		12. SPONSORING MILITARY ACTIVITY Department of the Navy (Office of Naval Research), Washington, D.C. 20360	
13. ABSTRACT Shipboard measurements of atmospheric potential gradient are discussed. A comparison is made at sea between the performance of a potential-measuring apparatus and a field mill. The design of electrometer input multistage voltage followers is presented as a solution to the degradation of insulators by the salt environment. A model is given which calculates from the ship's engine power and the relative wind vector the potential gradient due to the charged stack gas. A method is also described by which a reduction factor can be calculated so that the geometric distortion of a ship's superstructure is accounted for in potential-gradient measurements.			

14. KEY WORDS	LINK A		LINK B		LINK C	
	ROLE	WT	ROLE	WT	ROLE	WT
Potential gradient, atmospheric Voltage followers Atmospheric electricity Stack gas model Reduction factors						